PERGAMON

International Journal of Solids and Structures 37 (2000) 5061–5078

INTERNATIONAL JOURNAL OF SOLIDS and STRUCTURES

www.elsevier.com/locate/ijsolstr

Splitting the elastic strain energy in thin plates of a transversely isotropic material

Pericles S. Theocaris*, Dimitrios P. Sokolis

National Academy of Athens, P.O. Box 77230, 175 10, Athens, Greece

Received 10 September 1998; in revised form 10 February 1999

Abstract

In this paper, the elastic strain energy stored in thin plates of a transversely isotropic material is decomposed into distinct, non-interacting elements. Utilizing the characteristics of the elliptic paraboloid failure surface, which was previously shown to constitute an ideal criterion for yielding and failure of anisotropic media, and focusing our attention on transversely isotropic plates, it is proven that the total elastic strain energy density may be divided into discrete orthogonal parts. Moreover, applying the spectral decomposition principle on the compliance fourth-rank tensor **S** of transversely isotropic plates, orthogonal states of stress are obtained, each associated with a specific strain energy component. Both decompositions of the elastic strain energy suggested in this paper are energy equivalent and advantageous, exhibiting close resemblance with the splitting of the total elastic strain energy in dilatational and distortional constituents, valid only for isotropic materials.

Keywords: Orthogonality; Elastic strain energy; Elliptic paraboloid failure surface; Spectral decomposition; Transversely isotropic plates

1. Introduction

There have been a few attempts to prove that the strain energy in anisotropic materials may be split into two independent components, corresponding to dilatational and distortional types of energy. The first effort was unsuccessful (Olszak and Urbanowski, 1956) and led to the conclusion that, in general, no unique decomposition of the elastic energy is valid, since the anisotropic quantities are not in proportion to the associated isotropic ones. Therefore, the generalization of even the simplest failure criteria, such as the Huber–von Mises–Hencky criterion, to anisotropic media was not convincing.

* Corresponding author. Tel.: +30-1-324-3410; fax: +30-1-324-35170.

0020-7683/00/$ - see front matter
PII: S0020-7683(99)00153-5

Afterwards, a yield criterion of quadric form was offered for anisotropic bodies exhibiting both elastic and plastic anisotropy (Olszak and Ostrowska-Maciejewska, 1985), where the elastic anisotropy tensor had the same deviatoric eigenstates as the plastic one, the flow function remained invariant for a proportional increase of all normal stress components, but the Bauschinger effect was neglected.

It was Rychlewski (1984a), who introduced the notion of energy orthogonal states of stress for any initially or plastically anisotropic material. A stress state was defined to be energy orthogonal to another, if it did not perform along the deformations caused by the other. Furthermore, a theorem was proven, namely that a failure condition could be represented by a certain condition upon a linear superposition of energy orthogonal components of the total elastic strain energy, corresponding to uniquely determined for the given material paring-wise energy orthogonal, additive components of the total state of stress. Therefore, each quadratic criterion was shown to have a definite energy interpretation.

Rychlewski (1984b) also established the possibility of spectrally decomposing the elastic stiffness $\mathbf{C}$ and compliance $\mathbf{S}$ fourth-rank tensors. Earlier on, Srinivasan and Nigam (1969) as well as Walpole (1981, 1984) employed other decompositions on fourth-rank tensors, offering insight into the tensor structure, and facilitating operations between these tensors, such as calculations of inverses and products. However, important as they were for crystallographic applications, these decompositions were not of the spectral type, except in the trivial cases of isotropic and cubic symmetry.

The analysis initiated by Rychlewski was, subsequently, advanced (Theocaris and Philippidis, 1990, 1991), and the class of transversely isotropic media was examined specifically. Thus, the invariant parameters of the spectral decomposition of the compliance tensor $\mathbf{S}$ were determined, and the elastic potential of the transversely isotropic medium was granted an explicit decomposition in distinct elements, indicating the nonexistence of a sole dilatation energy component. Nonetheless, most of the experimental evidence today exists for plane-stress problems. Hence, the three-dimensional spectral decomposition was extended (Theocaris and Sokolis, 1998) to encompass the equally important two-dimensional equivalent, offering a possibility of characterization of the elastic properties under plane-stress situations.

In this paper, the elastic strain energy density of thin transversely isotropic plates is analyzed into autonomous components. Bearing in mind the consequential role undertaken by the total elastic strain energy density or parts of it in the formulation of failure criteria for isotropic solids, the necessity of obtaining analogous, more general types of decompositions of the strain energy is evident, for the definition of the respective criteria, which will be valid for anisotropic bodies. Accordingly, based on the geometrical features of the elliptic paraboloid failure surface, which was previously proven (Theocaris, 1987a, b; Theocaris and Philippidis, 1987) to be a convenient failure locus for a satisfactory description of the complex modes of failure of anisotropic materials, and confining our attention to transversely isotropic plates, it is shown that the elastic strain energy at the limit of failure is split into two energy parts, derived from orthogonal states of stress in such a manner that each component of stress in either energy part does not contribute to the other energy part. Furthermore, by spectrally expanding the compliance tensor $\mathbf{S}$, orthogonal states of stress are obtained, corresponding to distinct energy components. Both decompositions of the total elastic strain energy, proposed in this paper, are energy equivalent and advantageous, owing to the fact that they manifest similarities with the decomposition of the strain energy of isotropic bodies into dilatational and distortional elements, respectively.

2. The elliptic paraboloid failure surface and the decomposition of the elastic strain energy density

Modern failure criteria originate from Hill's criterion (Hill, 1948), which, in turn, was based on von Mises' initial definition of yielding and failure of anisotropic solids (von Mises, 1928). Nevertheless,

Hill's criterion did not incorporate important universal phenomena of the mechanical behavior of materials, such as the Bauschinger effect and others dependent on the strength differential effect. From the old generation of criteria, only the Coulomb criterion took into consideration the strength differential effect (Coulomb, 1773), by introducing the first stress invariant into its expression, thus, relating the dilatational and distortional types of strain energy, and realizing its contribution in the failure modes of materials. Improvement to the criteria of anisotropic bodies was offered by Hoffman's criterion, by adding the linear terms in the quadratic expression of Hill's criterion (Hoffman, 1967), therefore, presenting an improved version of Hill's criterion, which exhibited the strength differential effect.

Further improvement to the first typical yield and failure criteria was offered by two basic criteria, which were developed recently. These are the Tsai–Wu tensor failure polynomial (TFP) (Tsai and Wu, 1971) and the elliptic paraboloid failure surface (EPFS), which are based on Hill's criterion and its modification by Hoffman. Both are convenient for the description of the failure behavior of anisotropic media, complying with energy balance considerations and basic physical laws. However, despite the flexibility and elegance of the TFP-criterion, this necessitates meticulous and delicate experiments, as well as an extensive study based on Weibull's distribution theory, in order to determine appropriately the characteristic parameters defining the failure locus. Oppositely, the EPFS-criterion serves as a superb instrument for the precise evaluation of the effect of variation of one failure component on the values of the remaining ones.

Initially, the EPFS-criterion was introduced (Theocaris, 1986, 1987c) for the definition of the failure surface of isotropic materials, which exhibited the strength differential effect. This was defined by a parameter $R=\sigma_{OC}/\sigma_{OT}$, where σ_{OC} and σ_{OT} are the yield stresses in compression and tension, respectively, and the EPFS obtained the shape of a paraboloid of revolution surface. For orthotropic media (Theocaris, 1989), three different strength differential parameters were defined, $R_1=\sigma_{C1}/\sigma_{T1}$, $R_2=\sigma_{C2}/\sigma_{T2}$, $R_3=\sigma_{C3}/\sigma_{T3}$, with respect to six distinct strength parameters, three for tension and three for compression along the principal strength axes of the body. Finally, for transversely isotropic media with the σ_3-axis being the axis of symmetry, there were only two strength differential parameters $R_1=R_2$ and R_3. Furthermore, it is worthwhile pointing out that the axis of symmetry of the EPFS for both isotropic, transversely isotropic and orthotropic materials was parallel to the hydrostatic axis in the stress space, apart from the fact that all failure surfaces were paraboloids.

The EPFS-criterion was exhaustively compared in Theocaris (1994), with all other well-known failure tensor polynomial criteria. Moreover, the characteristics of the EPFS have been derived in previous papers (Theocaris 1987a, b; Theocaris and Philippidis, 1987). However, it is appropriate to briefly state these properties again here, since they constitute the basis for establishing the expressions of the strain energy components at failure. Consider a transversely isotropic body with failure tensors H_{ij} and h_i along the principal stress axes, where $i, j = 1, 2, 3$ and the 33-axis is presumed to be the strong axis of the medium. The components of the failure tensors are expressed by:

$$H_{ii}=\frac{1}{\sigma_{T_i}\sigma_{C_i}},\quad H_{ij}=\frac{1}{2}(H_{kk}-H_{ii}-H_{jj}), \tag{1a}$$

$$h_i=\frac{1}{\sigma_{T_i}}-\frac{1}{\sigma_{C_i}}=(\sigma_{C_i}-\sigma_{T_i})H_{ii}, \tag{1b}$$

where the repeated index convention does not apply, and the σ_{T_i} and σ_{C_i}-stresses express the tension, T, and compression, C, failure stresses in the i-direction. Then, the RHS of relations (1a) implies that the off-diagonal failure components H_{ij} are interrelated with the diagonal ones, this being a major advantage of the EPFS-criterion in comparison to all other FTP-criteria, in which the experimental

evaluation of the off-diagonal components presents insurmountable difficulties. Assuming, further, that the principal stress axes coincide with the material principal strength axes, the failure surface is expressed by (Theocaris, 1987a, c):

$$H_{11}(\sigma_1^2+\sigma_2^2)+H_{33}\sigma_3^2-(2H_{11}-H_{33})\sigma_1\sigma_2-H_{33}(\sigma_2\sigma_3+\sigma_3\sigma_1)+h_1(\sigma_1+\sigma_2)+h_3\sigma_3=1. \tag{2}$$

The quadric surface, represented by relation (2), is an elliptic paraboloid surface, which is symmetric with respect to the principal diagonal plane (σ_3, δ_{12}), containing the σ_3-axis and passing through the bisector δ_{12} of angle $\sigma_1\hat{O}\sigma_2$. Fig. 1 exhibits the elliptic paraboloid failure surface, whose axis of symmetry $KO'z'$ is parallel to the Oz-hydrostatic axis in the principal stress space (σ_1, σ_2, σ_3). The Cartesian reference system $Oxyz$ is formed by rotation of the (σ_1, σ_2, σ_3)-system, so that the Ox-axis becomes a bisector of the (σ_1, σ_2)-plane, the Oz-axis coincides with the hydrostatic axis, and the Oy-axis forms a tri-orthogonal system. In addition, the $Ox'y'z'$-system is formed from the $Oxyz$-system by translating the origin O to the new origin O' by a distance y_1. This distance y_1 between the hydrostatic axis and the axis of symmetry of the EPFS is given by:

$$y_1=\frac{\sqrt{6}}{9H_{33}}(h_1-h_3). \tag{3}$$

The cross-section of the EPFS by the principal plane (σ_1, σ_3) may be derived from relation (2), by setting $\sigma_2=0$. This substitution yields (Theocaris, 1988a, b):

$$H_{11}\sigma_1^2+H_{33}\sigma_{33}^2-H_{33}\sigma_1\sigma_3+h_1\sigma_1+h_3\sigma_3=1. \tag{4}$$

Relation (4) indicates that the intersection of the EPFS by the principal stress plane (σ_1, σ_3) is an ellipse (Fig. 2), whose center M has coordinates (σ_{1m}, σ_{3m}):

$$\sigma_{1m}=-\frac{(2h_1+h_3)}{4H_{11}-H_{33}}, \tag{5a}$$

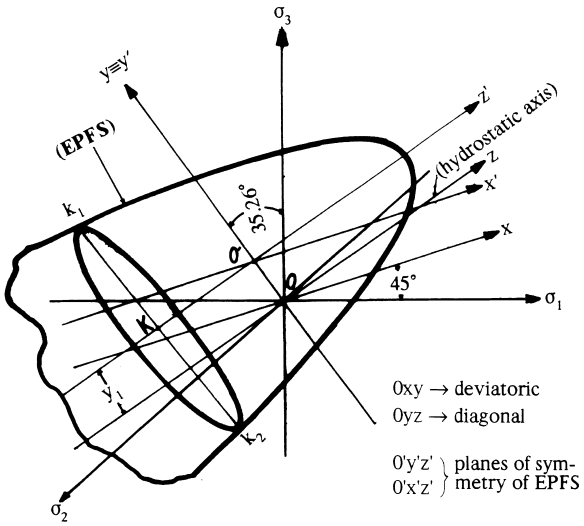

Fig. 1. Three-dimensional appearance of the elliptic paraboloid failure surface (EPFS) in the principal stress system (σ_1, σ_2, σ_3) and the Cartesian system $Ox'y'z'$, where the $O'z'$-axis is parallel to the hydrostatic axis Oz.

$$\sigma_{3m} = -\frac{(h_1 H_{33} + 2h_3 H_{11})}{H_{33}(4H_{11} - H_{33})}. \tag{5b}$$

Moreover, the angle λ_m of inclination of the polar radius OM is given by:

$$\lambda_m = \tan^{-1}\left[\frac{h_1 H_{33} + 2h_3 H_{11}}{H_{33}(2h_1 + h_3)}\right]. \tag{6}$$

The system of Cartesian coordinates ($M\Sigma_1$, Σ_3), to which this ellipse is central and symmetric, is defined by angle θ_1:

$$\theta_1 = \frac{1}{2}\tan^{-1}\left[\frac{H_{33}}{H_{11} - H_{33}}\right]. \tag{7}$$

In order to define the principal semi-axes α_{1M} and α_{3M} of the elliptic intersection of the EPFS by the principal plane (σ_1, σ_3), we need to evaluate the following quantities:

1. The determinant of the matrix of coefficients $\mathbf{A}_2$ of the second-degree terms of relation (4):

$$\mathbf{A}_2 = \begin{pmatrix} H_{33} & -\frac{H_{33}}{2} \\ -\frac{H_{33}}{2} & H_{11} \end{pmatrix}, \tag{8}$$

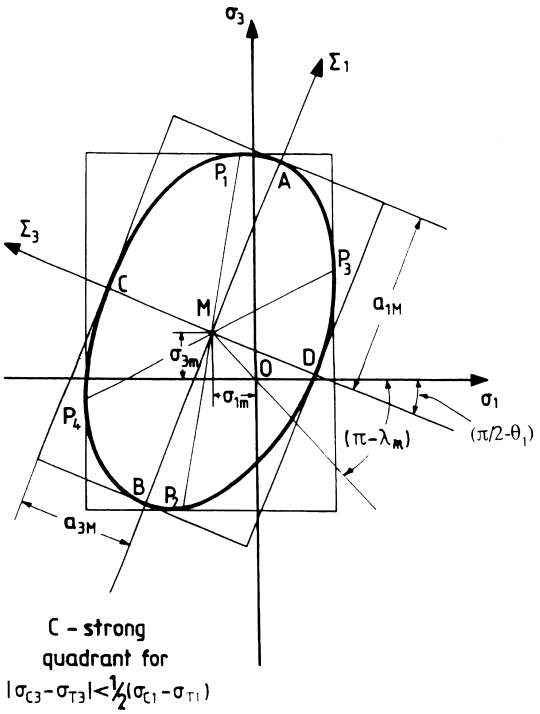

Fig. 2. Intersection of the elliptic paraboloid failure surface (EPFS) by the (σ_1, σ_3) principal stress plane for a transversely isotropic material.

which gives

$$\det\mathbf{A}_2 = \left(H_{11}H_{33} - \frac{H_{33}^2}{4}\right). \tag{9}$$

2. The determinant of the following matrix $\mathbf{A}_3$:

$$\mathbf{A}_3 = \begin{pmatrix} H_{33} & -\frac{H_{33}}{2} & \frac{h_3}{2} \\ -\frac{H_{33}}{2} & H_{11} & \frac{h_1}{2} \\ \frac{h_3}{2} & \frac{h_1}{2} & -1 \end{pmatrix} \tag{10}$$

yielding

$$\det\mathbf{A}_3 = -\det\mathbf{A}_2 - \tfrac{1}{4}(H_{33}h_1^2 + H_{11}h_3^2 + H_{33}h_1h_3). \tag{11}$$

3. The roots $\delta_{1,2}$ of the characteristic equation:

$$\delta^2 - \mathrm{tr}\mathbf{A}_2\delta + \det\mathbf{A}_2 = 0. \tag{12}$$

These roots are expressed by:

$$\delta_{1,2} = \tfrac{1}{2}\{(H_{11} + H_{33}) \pm [(H_{11} - H_{33})^2 + H_{33}^2]^{1/2}\}. \tag{13}$$

Then, the semi-axes α_{1M} and α_{3M} of the ellipse are given by:

$$(\alpha_{1M}, \alpha_{3M}) = \left(\frac{C}{\delta_{1,2}}\right)^{1/2} \tag{14a}$$

where

$$C = -\frac{\det\mathbf{A}_3}{\det\mathbf{A}_2}, \tag{14b}$$

and this concludes the description of the elliptic paraboloid failure locus for transversely isotropic materials.

Consider now two unit vectors $\mathbf{n}_\mathrm{p}$ and $\mathbf{n}_\mathrm{n}$, which are normal and parallel to the projection of the hydrostatic axis on the principal stress plane (σ_1, σ_3). These vectors are defined as follows (Fig. 3):

$$\mathbf{n}_\mathrm{p} = \left[-\frac{1}{\sqrt{2}}, \frac{1}{\sqrt{2}}\right]^\mathrm{T}, \tag{15a}$$

$$\mathbf{n}_\mathrm{n} = \left[\frac{1}{\sqrt{2}}, \frac{1}{\sqrt{2}}\right]^\mathrm{T}. \tag{15b}$$

According to the classical analysis for anisotropic media (Lekhnitskii, 1963), the principal stress–strain relations under plane stress conditions, $\sigma_2 = 0$, are given by:

$$\epsilon_1 = \frac{1}{E_T}\sigma_1 - \frac{\nu_L}{E_L}\sigma_3, \tag{16a}$$

$$\epsilon_2 = -\frac{\nu_T}{E_T}\sigma_1 - \frac{\nu_L}{E_L}\sigma_3, \tag{16b}$$

$$\epsilon_3 = \frac{1}{E_L}\sigma_3 - \frac{\nu_L}{E_L}\sigma_1, \tag{16c}$$

where E_L, E_T, ν_L and ν_T are the elastic constants along the longitudinal, denoted by subscript 'L', and transverse, denoted by subscript 'T', directions.

The projections of the stress vector $\boldsymbol{\sigma}$ along the unit vectors $\mathbf{n}_p$ and $\mathbf{n}_n$ in the (σ_1, σ_3)-plane are readily evaluated to be:

$$\boldsymbol{\sigma}_p = (\boldsymbol{\sigma}\cdot\mathbf{n}_p)\mathbf{n}_p = \left[\frac{\sigma_1-\sigma_3}{2}, -\frac{\sigma_1-\sigma_3}{2}\right]^T, \tag{17a}$$

$$\boldsymbol{\sigma}_n = (\boldsymbol{\sigma}\cdot\mathbf{n}_n)\mathbf{n}_n = \left[\frac{\sigma_1+\sigma_3}{2}, \frac{\sigma_1+\sigma_3}{2}\right]^T. \tag{17b}$$

In addition, the projections of the strain vector $\boldsymbol{\epsilon}$ along the unit vectors $\mathbf{n}_p$ and $\mathbf{n}_n$ in the (σ_1, σ_3)-plane are expressed by:

$$\boldsymbol{\epsilon}_p = (\boldsymbol{\epsilon}\cdot\mathbf{n}_p)\mathbf{n}_p = \left[-\frac{\sigma_3}{2}\left(\frac{1+\nu_L}{E_L}\right) + \frac{\sigma_1}{2}\left(\frac{1}{E_T}+\frac{\nu_L}{E_L}\right), \frac{\sigma_3}{2}\left(\frac{1+\nu_L}{E_L}\right) - \frac{\sigma_1}{2}\left(\frac{1}{E_T}+\frac{\nu_L}{E_L}\right)\right]^T, \tag{18a}$$

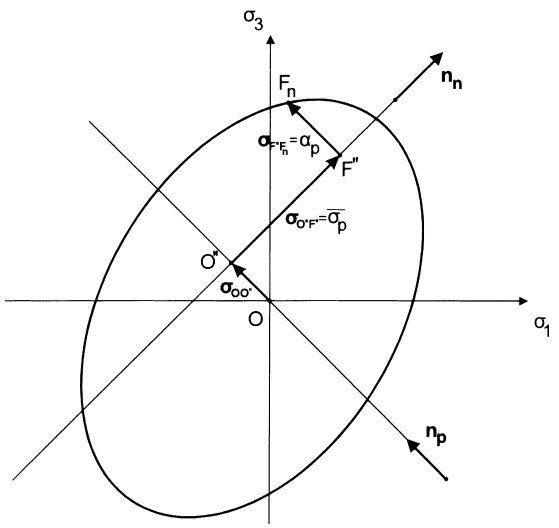

Fig. 3. The unit vectors $\mathbf{n}_n$ and $\mathbf{n}_p$ are parallel to the projections of the hydrostatic axis and its normal on the principal (σ_1, σ_3) stress plane.

$$\boldsymbol{\epsilon}_{\mathrm{n}} = (\boldsymbol{\epsilon}\cdot\mathbf{n}_{\mathrm{n}})\mathbf{n}_{\mathrm{n}} = \left[\frac{\sigma_3}{2}\left(\frac{1-\nu_{\mathrm{L}}}{E_{\mathrm{L}}}\right)+\frac{\sigma_1}{2}\left(\frac{1}{E_{\mathrm{T}}}-\frac{\nu_{\mathrm{L}}}{E_{\mathrm{L}}}\right),\ \frac{\sigma_3}{2}\left(\frac{1-\nu_{\mathrm{L}}}{E_{\mathrm{L}}}\right)+\frac{\sigma_1}{2}\left(\frac{1}{E_{\mathrm{T}}}-\frac{\nu_{\mathrm{L}}}{E_{\mathrm{L}}}\right)\right]^{\mathrm{T}}. \tag{18b}$$

The total elastic strain energy density 2 $T(\boldsymbol{\sigma})$ is expressed by:

$$2T(\boldsymbol{\sigma}) = \boldsymbol{\sigma}\cdot\boldsymbol{\epsilon} = (\boldsymbol{\sigma}_{\mathrm{p}}+\boldsymbol{\sigma}_{\mathrm{n}})\cdot(\boldsymbol{\epsilon}_{\mathrm{p}}+\boldsymbol{\epsilon}_{\mathrm{n}}) = \boldsymbol{\sigma}_{\mathrm{p}}\cdot\boldsymbol{\epsilon}_{\mathrm{p}}+\boldsymbol{\sigma}_{\mathrm{n}}\cdot\boldsymbol{\epsilon}_{\mathrm{n}}, \tag{19}$$

since $\boldsymbol{\sigma}_{\mathrm{p}}\cdot\boldsymbol{\epsilon}_{\mathrm{n}}=0=\boldsymbol{\sigma}_{\mathrm{n}}\cdot\boldsymbol{\epsilon}_{\mathrm{p}}$.

Then, the two parallel and normal orthogonal components 2 $T_i(\boldsymbol{\sigma})=\boldsymbol{\sigma}_i\times\boldsymbol{\epsilon}_i$, i = p, n into which the total elastic strain energy is analyzed are expressed by:

$$2T_{\mathrm{p}}(\boldsymbol{\sigma}) = \frac{\sigma_1^2}{2}\left(\frac{1}{E_{\mathrm{T}}}+\frac{\nu_{\mathrm{L}}}{E_{\mathrm{L}}}\right)+\frac{1}{2}\left(\frac{1+\nu_{\mathrm{L}}}{E_{\mathrm{L}}}\right)\sigma_3^2-\frac{1}{2}\left[\frac{1}{E_{\mathrm{T}}}+\left(\frac{1+2\nu_{\mathrm{L}}}{E_{\mathrm{L}}}\right)\right]\sigma_1\sigma_3, \tag{20a}$$

$$2T_{\mathrm{n}}(\boldsymbol{\sigma}) = (\sigma_1+\sigma_3)\left[\frac{\sigma_3}{2}\left(\frac{1-\nu_{\mathrm{L}}}{E_{\mathrm{L}}}\right)+\frac{\sigma_1}{2}\left(\frac{1}{E_{\mathrm{T}}}-\frac{\nu_{\mathrm{L}}}{E_{\mathrm{L}}}\right)\right]. \tag{20b}$$

Relations (20) assert that the elastic strain energy components are independent of the value of the transverse Poisson's ratio ν_{T}, a fact which must be taken into account in the manufacture of thin plates of a transversely isotropic medium.

3. Spectral decomposition of the elastic strain energy density

Consider the spectral decomposition of the compliance fourth-rank tensor $\mathbf{S}$ of a transversely isotropic linear elastic plate. The stress $\boldsymbol{\sigma}$ and strain $\boldsymbol{\epsilon}$ second-rank tensors are referred to a Cartesian coordinate system, adjusted along the principal material directions, with the 33-axis normal to the isotropic, transverse plane. The eigenvalues λ_m, m = 1,...,3 of the square matrix of rank three, corresponding to tensor $\mathbf{S}$, are given by (Theocaris and Sokolis, 1998):

$$\lambda_1 = \frac{1}{2E_{\mathrm{L}}}+\frac{1}{2E_{\mathrm{T}}}+\left[\left(\frac{1}{2E_{\mathrm{L}}}-\frac{1}{2E_{\mathrm{T}}}\right)^2+\frac{\nu_{\mathrm{L}}^2}{E_{\mathrm{L}}^2}\right]^{1/2}, \tag{21a}$$

$$\lambda_2 = \frac{1}{2E_{\mathrm{L}}}+\frac{1}{2E_{\mathrm{T}}}-\left[\left(\frac{1}{2E_{\mathrm{L}}}-\frac{1}{2E_{\mathrm{T}}}\right)^2+\frac{\nu_{\mathrm{L}}^2}{E_{\mathrm{L}}^2}\right]^{1/2}, \tag{21b}$$

$$\lambda_3 = \frac{1}{2G_{\mathrm{L}}}. \tag{21c}$$

Subscripts 'T' and 'L' in the engineering elastic constants of relations (21) denote the transverse isotropic plane and the orthogonal, longitudinal plane, containing the axis of elastic symmetry.

The associated idempotent fourth-rank tensors $\mathbf{E}_m$, m = 1,...,3 decompose spectrally the compliance fourth-rank tensor $\mathbf{S}$ and the unit element $\mathbf{I}$ of the fourth-rank symmetric tensor space, via the following relations:

$$\mathbf{S} = \lambda_1\mathbf{E}_1+\lambda_2\mathbf{E}_2+\lambda_3\mathbf{E}_3, \tag{22a}$$

$$\mathbf{I} = \mathbf{E}_1 + \mathbf{E}_2 + \mathbf{E}_3. \tag{22b}$$

Secondly, the idempotent tensors $\mathbf{E}_m$ satisfy the following set of equations:

$$\mathbf{E}_m \cdot \mathbf{E}_n = 0, \quad m \neq n, \tag{23a}$$

$$\mathbf{E}_m \cdot \mathbf{E}_m = \mathbf{E}_m. \tag{23b}$$

Besides, if the stress states $\overline{\boldsymbol{\sigma}_m}$ constitute the second-rank eigentensors of the compliance tensor $\mathbf{S}$, they need to satisfy the eigenvalue equation:

$$\mathbf{S} \cdot \overline{\boldsymbol{\sigma}_m} = \lambda_m \overline{\boldsymbol{\sigma}_m}, \tag{24}$$

with index m varying between 1 and 3, and the eigenvalues λ_m being offered in terms of relations (21). Stress eigentensors $\overline{\boldsymbol{\sigma}_m}$ are derived by the orthogonal projection of a second-rank symmetric tensor $\boldsymbol{\sigma}$ on the subspaces of the second-rank symmetric tensor space produced by the idempotent tensors $\mathbf{E}_m$, as follows:

$$\overline{\boldsymbol{\sigma}_m} = \mathbf{E}_m \cdot \boldsymbol{\sigma}, \quad m = 1, \ldots, 3, \tag{25}$$

where $\boldsymbol{\sigma}$ is the contracted stress tensor:

$$\boldsymbol{\sigma} = [\sigma_1, \sigma_3, \sigma_{13}]^{\mathrm{T}}. \tag{26}$$

According to relations (25), it is found that:

$$\overline{\boldsymbol{\sigma}_1} = (\cos \omega_{\mathrm{p}}(\sigma_1) + \sin \omega_{\mathrm{p}}(\sigma_3))[\cos \omega_{\mathrm{p}}, \ \sin \omega_{\mathrm{p}}, 0]^{\mathrm{T}}, \tag{27a}$$

$$\overline{\boldsymbol{\sigma}_2} = (\sin \omega_{\mathrm{p}}(\sigma_1) - \cos \omega_{\mathrm{p}}(\sigma_3))[\sin \omega_{\mathrm{p}}, \ -\cos \omega_{\mathrm{p}}, 0]^{\mathrm{T}}, \tag{27b}$$

$$\overline{\boldsymbol{\sigma}_3} = [0, 0, \sigma_{13}]^{\mathrm{T}}, \tag{27c}$$

where ω_{p} is referred to as the plane eigenangle and is defined according to the following formula:

$$\tan 2\omega_{\mathrm{p}} = -\frac{2\nu_{\mathrm{L}}}{E_{\mathrm{L}}} \Big/ \left(\frac{1}{E_{\mathrm{T}}} - \frac{1}{E_{\mathrm{L}}}\right). \tag{28}$$

The $\overline{\boldsymbol{\sigma}_1}$-eigenstate represents a superposition of a tension stress state in the 11-axis with a tension along the infinite symmetry 33-axis of the plate, whereas the $\overline{\boldsymbol{\sigma}_2}$-eigenstate replaces the uniaxial tension by uniaxial compression along the symmetry axis. Finally, the $\overline{\boldsymbol{\sigma}_3}$-eigenstate is a simple shear stress state. In addition, relations (27) imply that the stress eigenstates break down the generic stress tensor $\boldsymbol{\sigma}$ into three orthogonal components $\overline{\boldsymbol{\sigma}_1}$, $\overline{\boldsymbol{\sigma}_2}$ and $\overline{\boldsymbol{\sigma}_3}$. It should be taken into consideration that the components of the $\overline{\boldsymbol{\sigma}_1}$- and $\overline{\boldsymbol{\sigma}_2}$-eigentensors (Fig. 4) are dependent upon the value of the plane eigenangle ω_{p}, given by relation (28), and the engineering elastic constants of the material, whereas the third eigentensor $\overline{\boldsymbol{\sigma}_3}$ is constant for the whole class of transversely isotropic media.

In addition, the total elastic strain energy density may be decomposed in three distinct energy components, each one associated with the respective stress eigentensor:

$$2T(\boldsymbol{\sigma}) = T_1(\boldsymbol{\sigma}) + T_2(\boldsymbol{\sigma}) + T_3(\boldsymbol{\sigma}), \tag{29}$$

where

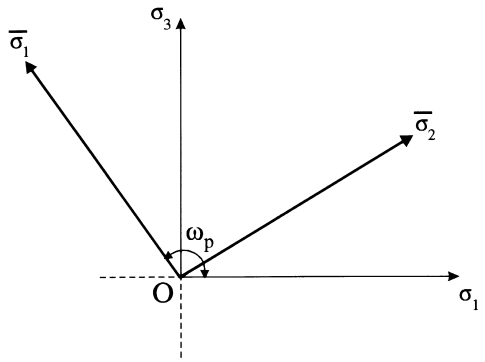

Fig. 4. Geometric representation of the eigentensors $\overline{\boldsymbol{\sigma}_1}$ and $\overline{\boldsymbol{\sigma}_2}$ of the compliance fourth-rank tensor **S** for transversely isotropic plates on the principal stress plane (σ_1, σ_3).

$$T_m(\boldsymbol{\sigma}) = \lambda_m(\overline{\boldsymbol{\sigma}_m} \cdot \overline{\boldsymbol{\sigma}_m}), \quad m = 1, \ldots, 3. \tag{30}$$

Thus, the following expressions are obtained for the strain-energy density constituents of a transversely isotropic plate:

$$T_1(\boldsymbol{\sigma}) = \left\{ \frac{1}{2E_{\mathrm{L}}} + \frac{1}{2E_{\mathrm{T}}} + \left[\left(\frac{1}{2E_{\mathrm{L}}} - \frac{1}{2E_{\mathrm{T}}} \right)^2 + \frac{\nu_{\mathrm{L}}^2}{E_{\mathrm{L}}^2} \right]^{1/2} \right\} [\cos \omega_{\mathrm{p}}(\sigma_1) + \sin \omega_{\mathrm{p}}(\sigma_3)]^2, \tag{31a}$$

$$T_2(\boldsymbol{\sigma}) = \left\{ \frac{1}{2E_{\mathrm{L}}} + \frac{1}{2E_{\mathrm{T}}} - \left[\left(\frac{1}{2E_{\mathrm{L}}} - \frac{1}{2E_{\mathrm{T}}} \right)^2 + \frac{\nu_{\mathrm{L}}^2}{E_{\mathrm{L}}^2} \right]^{1/2} \right\} [\sin \omega_{\mathrm{p}}(\sigma_1) - \cos \omega_{\mathrm{p}}(\sigma_3)]^2, \tag{31b}$$

$$T_3(\boldsymbol{\sigma}) = \frac{1}{G_{\mathrm{L}}} (\sigma_{13})^2. \tag{31c}$$

Relations (31) state that the two strain energy components $T_1(\boldsymbol{\sigma})$ and $T_2(\boldsymbol{\sigma})$ depend upon the value of the plane eigenangle ω_{p}, given by relation (28), and correspond to a mixture of distortional and voluminal energy. The third energy component $T_3(\boldsymbol{\sigma})$ is independent of the value of the plane eigenangle ω_{p}, and is solely associated with distortional energy.

4. Orthogonal components of the elastic strain energy density in the principal stress plane

Relations (20) and (31), which are orthonormal in the sense of their scalar products, express the strain energy density components obtained from the two decompositions of the total strain energy proposed in this paper. Relations (20) express the components of the elastic strain energy density attained from orthogonal stresses and strains along the projection of the hydrostatic axis and its normal on the principal stress plane (σ_1, σ_3). Relations (31) yield the strain energy parts acquired from the more general splitting of the strain energy, based on the spectral decomposition of the compliance tensor **S** for transversely isotropic plates. Direct inspection of Eqs. (20) and (31) reveals that the energy density elements are expressed in terms of stresses σ_1 and σ_3 of a generic point on the stress plane. If this point

is taken on the EPFS, it is essential that the stress coordinates are defined in terms of relation (4), which expresses the defining equation of the EPFS on the (σ_1, σ_3)-plane.

Taking advantage of the geometrical features of the EPFS, a direct analysis of the stress vector $\boldsymbol{\sigma}_{F_n}$ corresponding to an arbitrary point F_n of the failure surface is utilized, by splitting it into three components, namely (Fig. 5):

$$\boldsymbol{\sigma}_{F_n} = \boldsymbol{\sigma}_{OO'} + \boldsymbol{\sigma}_{O'F} + \boldsymbol{\sigma}_{FF_n}, \tag{32}$$

in which the stress vectors $\boldsymbol{\sigma}_{OO'}$ and $\boldsymbol{\sigma}_{FF_n}$ are parallel to the deviatoric plane $(\sigma_1+\sigma_2+\sigma_3)=0$, whereas the $\boldsymbol{\sigma}_{O'F}$-vector is parallel to the hydrostatic axis z. Moreover, the $\boldsymbol{\sigma}_{OO'}$-vector is independent of the position of point F_n and depends only on the characteristics of the EPFS.

Nevertheless, the splitting of the stress vector $\boldsymbol{\sigma}_{F_n}$ described above is convenient for three-dimensional loading of the structure. For the case of thin plates of a transversely isotropic medium, attention must be restricted to the principal stress plane (σ_1, σ_3). In this case, the stress vector, lying on the elliptic intersection of the EPFS by the principal plane (σ_1, σ_3), is analyzed into three constituents, these being the projections of the three vector components $\boldsymbol{\sigma}_{OO'}$, $\boldsymbol{\sigma}_{O'F}$ and $\boldsymbol{\sigma}_{FF_n}$ on the (σ_1, σ_3)-plane, that is $\boldsymbol{\sigma}_{OO''}$, $\boldsymbol{\sigma}_{O''F''}$ and $\boldsymbol{\sigma}_{F''F_n}$. Therefore, points O' and F are projected to points O'' and F'' on the principal stress plane (σ_1, σ_3) (Fig. 3). In addition, stresses $\boldsymbol{\sigma}_{O''F''}$ and $\boldsymbol{\sigma}_{F''F_n}$ are denoted by $\overline{\sigma_p}$ and α_p, respectively.

Consider first the strain energy density $2\,T(\boldsymbol{\sigma}_{OO''})$, corresponding to stress $\boldsymbol{\sigma}_{OO''}$ and strain $\boldsymbol{\epsilon}_{OO''}$-vectors (Fig. 6). The components of the $\boldsymbol{\sigma}_{OO''}$-vector are expressed by:

$$\sigma_1 = \frac{2(h_3 - h_1)}{9H_{33}}, \quad \sigma_3 = \frac{2(h_1 - h_3)}{9H_{33}}. \tag{33}$$

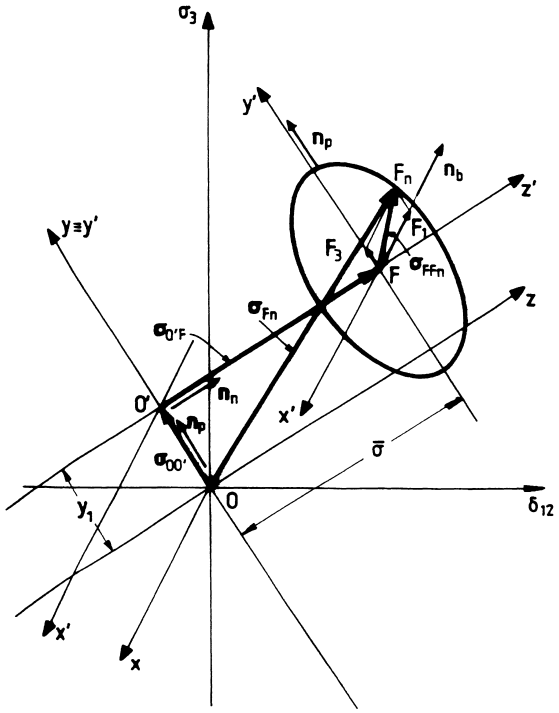

Fig. 5. The splitting of the stress vector $\boldsymbol{\sigma}_{F_n}$ of a generic point on the EPFS by the three components $\boldsymbol{\sigma}_{OO'}$, $\boldsymbol{\sigma}_{O'F}$ and $\boldsymbol{\sigma}_{FF_n}$.

Then, the parallel, 2 $T_{\mathrm{p}}(\boldsymbol{\sigma}_{OO''})$, and normal, 2 $T_{\mathrm{n}}(\boldsymbol{\sigma}_{OO''})$, parts of the total elastic strain energy density, defined by relations (20), are readily determined to be:

$$2T_{\mathrm{p}}(\boldsymbol{\sigma}_{OO''}) = \frac{4}{81}\left[\frac{1}{E_{\mathrm{T}}} + \left(\frac{1+2\nu_{\mathrm{L}}}{E_{\mathrm{L}}}\right)\right]\left(\frac{h_1 - h_3}{H_{33}}\right)^2, \tag{34a}$$

$$2T_{\mathrm{n}}(\boldsymbol{\sigma}_{OO''}) = 0. \tag{34b}$$

Moreover, consider the elastic strain energy density 2 $T(\boldsymbol{\sigma}_{OF''})$, performed by the stress vector $\boldsymbol{\sigma}_{OF''}$ (Fig. 6). The components of the $\boldsymbol{\sigma}_{OF''}$-vector are defined as:

$$\sigma_1 = \frac{2(h_3 - h_1)}{9H_{33}} + \frac{\overline{\sigma_{\mathrm{p}}}}{\sqrt{2}}, \quad \sigma_3 = \frac{2(h_1 - h_3)}{9H_{33}} + \frac{\overline{\sigma_{\mathrm{p}}}}{\sqrt{2}}. \tag{35}$$

The parallel, 2 $T_{\mathrm{p}}(\boldsymbol{\sigma}_{OF''})$, and normal, 2 $T_{\mathrm{n}}(\boldsymbol{\sigma}_{OF''})$, components of the elastic strain energy density are the expressed as follows

$$2T_{\mathrm{p}}(\boldsymbol{\sigma}_{OF''}) = 2T_{\mathrm{p}}(\boldsymbol{\sigma}_{OO''}) + \frac{\sqrt{2}}{9}\left(\frac{1}{E_{\mathrm{L}}} - \frac{1}{E_{\mathrm{T}}}\right)\left(\frac{h_1 - h_3}{H_{33}}\right)\overline{\sigma_{\mathrm{p}}}, \tag{36a}$$

$$2T_{\mathrm{n}}(\boldsymbol{\sigma}_{OF''}) = \frac{1}{2}\left[\frac{1}{E_{\mathrm{T}}} + \left(\frac{1-2\nu_{\mathrm{L}}}{E_{\mathrm{L}}}\right)\right]\overline{\sigma}_{\mathrm{p}}^2 + \frac{\sqrt{2}}{9}\left(\frac{1}{E_{\mathrm{L}}} - \frac{1}{E_{\mathrm{T}}}\right)\left(\frac{h_1 - h_3}{H_{33}}\right)\overline{\sigma_{\mathrm{p}}}. \tag{36b}$$

The first RHS term, 2 $T_{\mathrm{p}}(\boldsymbol{\sigma}_{OO''})$, of relation (36a) is equal to the strain energy performed in loading the structure by stress $\boldsymbol{\sigma}_{OO''}$ and the strain component $(\boldsymbol{\epsilon}_{OO''})_{\mathrm{p}}$, whereas the second term, denoted by 2 $T_{\mathrm{p}}(\boldsymbol{\sigma}_{O''F''})$, equals the strain energy produced by stress $\boldsymbol{\sigma}_{OO''}$ and the component of strain $(\boldsymbol{\epsilon}_{O''F''})_{\mathrm{p}}$. In addition, the first RHS term of relation (36b) equals the strain energy created by stress $\boldsymbol{\sigma}_{O''F''}$ and the component of strain $(\boldsymbol{\epsilon}_{OO''})_{\mathrm{n}}$, and the second term represents the strain energy produced by hydrostatic stress $\boldsymbol{\sigma}_{O''F''}$ and the component of strain $(\boldsymbol{\epsilon}_{O''F''})_{\mathrm{n}}$ (Fig. 6).

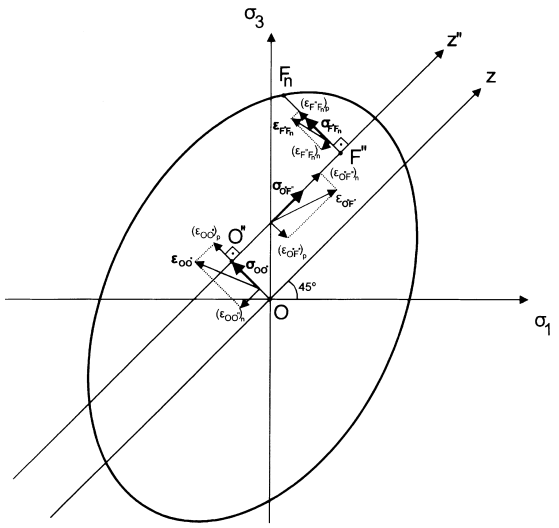

Fig. 6. The vector analysis of the first loading path on the principal stress plane (σ_1, σ_3).

Finally, regarding the elastic strain energy density $2\,T(\boldsymbol{\sigma}_{F_n})$, performed by the stress vector $\boldsymbol{\sigma}_{F_n}$ (Fig. 6), the components of the $\boldsymbol{\sigma}_{F_n}$-vector are given by:

$$\sigma_1 = \frac{2(h_3 - h_1)}{9H_{33}} + \frac{\overline{\sigma_p}}{\sqrt{2}} - \frac{\alpha_p}{\sqrt{2}}, \quad \sigma_3 = \frac{2(h_1 - h_3)}{9H_{33}} + \frac{\overline{\sigma_p}}{\sqrt{2}} + \frac{\alpha_p}{\sqrt{2}}. \tag{37}$$

The parallel, $T_p(\boldsymbol{\sigma}_{F_n})$, and normal, $T_n(\boldsymbol{\sigma}_{F_n})$, constituents of the elastic strain energy density are then found to be:

$$2T_p(\boldsymbol{\sigma}_{F_n}) = 2T_p(\boldsymbol{\sigma}_{OO''}) + 2T_p(\boldsymbol{\sigma}_{O''F''}) + \frac{1}{2}\left[\frac{1}{E_T} + \left(\frac{1+2\nu_L}{E_L}\right)\right]\alpha_p^2 + \frac{2\sqrt{2}}{9}\left[\frac{1}{E_T} + \left(\frac{1+2\nu_L}{E_L}\right)\right] \times \left(\frac{h_1 - h_3}{H_{33}}\right)\alpha_p + \frac{1}{2}\left(\frac{1}{E_L} - \frac{1}{E_T}\right)\overline{\sigma_p}\alpha_p, \tag{38a}$$

$$2T_n(\boldsymbol{\sigma}_{F_n}) = 2T_n(\boldsymbol{\sigma}_{O''F''}) + \frac{1}{2}\left(\frac{1}{E_L} - \frac{1}{E_T}\right)\overline{\sigma_p}\alpha_p, \tag{38b}$$

where $T_p(\boldsymbol{\sigma}_{OO''})$, $T_p(\boldsymbol{\sigma}_{O''F''})$, and $T_n(\boldsymbol{\sigma}_{O''F''})$ are defined in relations (36). The third term in relation (38a) represents the strain energy produced by stress $\boldsymbol{\sigma}_{F''F_n}$ and the component of strain $(\boldsymbol{\epsilon}_{F''F_n})_p$, whereas the fourth term is equal to the strain energy performed by stress $\boldsymbol{\sigma}_{OO''}$ and strain component $(\boldsymbol{\epsilon}_{F''F_n})_p$, as well as the strain energy performed by stress $\boldsymbol{\sigma}_{F''F_n}$ and the strain component $(\boldsymbol{\epsilon}_{OO''})_p$, and the fifth term is performed by stress $\boldsymbol{\sigma}_{F''F_n}$ and the strain component $(\boldsymbol{\epsilon}_{O''F''})_p$. Finally, the second term in relation (38b) denotes the strain energy produced by stress $\boldsymbol{\sigma}_{O''F''}$ and the component of strain $(\boldsymbol{\epsilon}_{F''F_n})_n$ (Fig. 6).

In Section 3 of this paper, the spectral decomposition of the compliance **S** fourth-rank tensor for transversely isotropic plates was shown to propose a decomposition of the elastic strain energy density into two constituents, $T_1(\boldsymbol{\sigma})$ and $T_2(\boldsymbol{\sigma})$, corresponding to the two stress eigenstates $\overline{\boldsymbol{\sigma}_1}$ and $\overline{\boldsymbol{\sigma}_2}$, of the compliance tensor **S** on the principal stress plane (σ_1, σ_3). It is of interest, at this point, to determine the strain energy components corresponding to the spectral decomposition of the elastic strain energy and compare the results with the ones obtained above, for the decomposition of strain energy described in Section 2.

Consider first the spectral decomposition of the strain energy $2\,T(\boldsymbol{\sigma}_{OO''})$, corresponding to stress $\boldsymbol{\sigma}_{OO''}$ (Fig. 7), defined by relations (33). The components $T_1(\boldsymbol{\sigma}_{OO''})$ and $T_2(\boldsymbol{\sigma}_{OO''})$ of the elastic strain energy density, due to the two stress eigenstates $\overline{\boldsymbol{\sigma}_1}$ and $\overline{\boldsymbol{\sigma}_2}$, are expressed as follows:

$$T_1(\boldsymbol{\sigma}_{OO''}) = \frac{4}{81\Gamma}\left(\frac{h_1 - h_3}{H_{33}}\right)^2 \times (\Gamma^2 + A\Gamma + B\Gamma + 2\nu_L AB + 2\nu_L B^2 + 2\nu_L B\Gamma), \tag{39a}$$

$$T_2(\boldsymbol{\sigma}_{OO''}) = \frac{4}{81\Gamma}\left(\frac{h_1 - h_3}{H_{33}}\right)^2 \times (-\Gamma^2 + A\Gamma + B\Gamma - 2\nu_L AB - 2\nu_L B^2 + 2\nu_L B\Gamma), \tag{39b}$$

where quantities A, B and Γ are defined by:

$$A = \frac{1}{2E_T}, \quad B = \frac{1}{2E_L}, \quad \Gamma = \left[\left(\frac{1}{2E_T} - \frac{1}{2E_L}\right)^2 + \frac{\nu_L^2}{E_L^2}\right]^{1/2} = [(A-B)^2 + 4\nu_L^2 B^2]^{1/2}. \tag{40}$$

It is thus concluded that the $\overline{\boldsymbol{\sigma}_1}$- and $\overline{\boldsymbol{\sigma}_2}$-eigenstates contribute to the work done in loading the structure from the origin O to point O'', via point M'' along the directions of the $\overline{\boldsymbol{\sigma}_1}$- and $\overline{\boldsymbol{\sigma}_2}$-eigenvectors (Fig. 7).

Also consider the decomposition of the elastic strain energy density 2 $T(\boldsymbol{\sigma}_{O''F''})$, which is performed by stress $\boldsymbol{\sigma}_{O''F''}$ (Fig. 7), defined according to relations (35). The components $T_1(\boldsymbol{\sigma}_{O''F''})$ and $T_2(\boldsymbol{\sigma}_{O''F''})$ of the elastic strain energy density are expressed, in terms of quantities A, B and Γ, by:

$$T_1(\boldsymbol{\sigma}_{OF''}) = T_1(\boldsymbol{\sigma}_{OO''}) + \frac{\overline{\sigma}_p^2}{2\Gamma} \times (\Gamma^2 + A\Gamma + B\Gamma - 2\nu_L AB - 2\nu_L B^2 - 2\nu_L B\Gamma) + \frac{\sqrt[2]{2\sigma_p}}{9\Gamma}\left(\frac{h_1 - h_3}{H_{33}}\right) \times (B^2 - A^2 - A\Gamma + B\Gamma), \tag{41a}$$

$$T_2(\boldsymbol{\sigma}_{OF''}) = T_2(\boldsymbol{\sigma}_{OO''}) + \frac{\overline{\sigma}_p^2}{2\Gamma} \times (-\Gamma^2 + A\Gamma + B\Gamma + 2\nu_L AB + 2\nu_L B^2 - 2\nu_L B\Gamma) + \frac{\sqrt[2]{2\sigma_p}}{9\Gamma}\left(\frac{h_1 - h_3}{H_{33}}\right) \times (A^2 - B^2 - A\Gamma + B\Gamma). \tag{41b}$$

The first RHS terms of relations (41) correspond to 2 $T(\boldsymbol{\sigma}_{OO''})$, whereas the second and third terms express the strain energy density 2 $T(\boldsymbol{\sigma}_{O''F''})$. Thus, the $\overline{\boldsymbol{\sigma}_1}$- and $\overline{\boldsymbol{\sigma}_2}$-eigenstates contribute to the work done in loading the structure from point O'' to point F'', via point K'' along the direction of the $\overline{\boldsymbol{\sigma}_1}$- and $\overline{\boldsymbol{\sigma}_2}$-eigenvectors (Fig. 7).

Consider finally, the spectral decomposition of the elastic strain energy 2 $T(\boldsymbol{\sigma}_{F''F_n})$, which is performed by stress $\boldsymbol{\sigma}_{F''F_n}$ (Fig. 7), expressed by relations (37). The components $T_1(\boldsymbol{\sigma}_{F''F_n})$ and $T_2(\boldsymbol{\sigma}_{F''F_n})$ of the elastic strain energy density, when expressed in terms of quantities A, B and Γ, are given by:

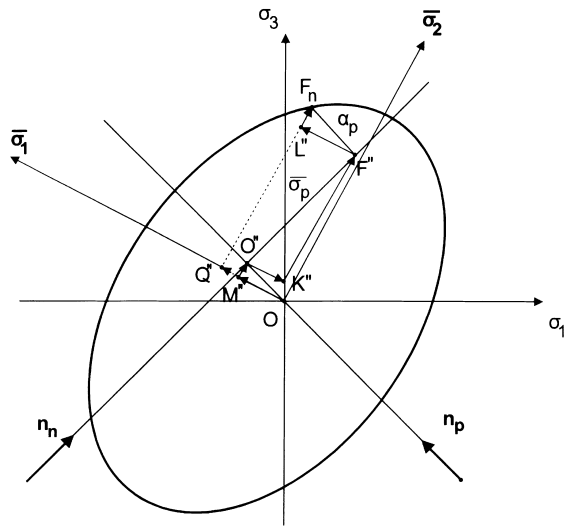

Fig. 7. The vector analysis of the second and third loading paths on the principal stress plane (σ_1, σ_3) along the directions of vectors $\overline{\boldsymbol{\sigma}_1}$ and $\overline{\boldsymbol{\sigma}_2}$, which constitute the stress eigentensors of the compliance tensor $\mathbf{S}$ for transversely isotropic plates.

$$T_1(\boldsymbol{\sigma}_{F_n}) = T_1(\boldsymbol{\sigma}_{OO''}) + T_1(\boldsymbol{\sigma}_{O''F''}) + \frac{\overline{\sigma_p}\alpha_p}{\Gamma} \times (B^2 - A^2 - A\Gamma + B\Gamma) + \left[\frac{\alpha_p^2}{2\Gamma} + \frac{2\sqrt{2}\alpha_p}{9\Gamma}\left(\frac{h_1 - h_3}{H_{33}}\right)\right] \times (\Gamma^2 + A\Gamma + B\Gamma + 2\nu_L AB + 2\nu_L B^2 + 2\nu_L B\Gamma), \tag{42a}$$

$$T_2(\boldsymbol{\sigma}_{F_n}) = T_2(\boldsymbol{\sigma}_{OO''}) + T_1(\boldsymbol{\sigma}_{O''F''}) + \frac{\overline{\sigma_p}\alpha_p}{\Gamma} \times (-B^2 + A^2 - A\Gamma + B\Gamma) + \left[\frac{\alpha_p^2}{2\Gamma} + \frac{2\sqrt{2}\alpha_p}{9\Gamma}\left(\frac{h_1 - h_3}{H_{33}}\right)\right] \times (-\Gamma^2 + A\Gamma + B\Gamma - 2\nu_L AB + 2\nu_L B^2 + 2\nu_L B\Gamma). \tag{42b}$$

It is readily noted that the first RHS terms of relations (42) denote 2 $T(\boldsymbol{\sigma}_{OO''})$, the second terms indicate the strain energy 2 $T(\boldsymbol{\sigma}_{O''F''})$, and finally the third and fourth terms are associated with the strain energy 2 $T(\boldsymbol{\sigma}_{F''F_n})$. Concluding, the $\overline{\boldsymbol{\sigma}_1}$- and $\overline{\boldsymbol{\sigma}_2}$-eigenstates contribute to the work done in loading the structure from point F'' to point F_n, via point L'', along the directions of the $\overline{\boldsymbol{\sigma}_1}$- and $\overline{\boldsymbol{\sigma}_2}$-eigenvectors (Fig. 7).

5. Discussion

In this paper, two ways were suggested for the partition of the elastic strain energy density of transversely isotropic plates into distinct elements. Utilizing the geometrical attributes of the elliptic paraboloid failure surface, which has been proven to be a suitable failure locus for characterizing satisfactorily the complex modes of failure of anisotropic media, and restraining our attention to thin plates of a transversely isotropic medium, it was proven that the total elastic strain energy at the limit of failure may be decomposed into two non-interacting strain energy components, $T_p(\boldsymbol{\sigma})$ and $T_n(\boldsymbol{\sigma})$, acquired from orthogonal states of stress.

The two components, $T_p(\boldsymbol{\sigma})$ and $T_n(\boldsymbol{\sigma})$, of the strain energy derived are orthogonal, since their scalar products lie the first normal and the second parallel to the hydrostatic axis. However, it should be made clear that, contrariwise to the case of isotropic media, these strain energies do not correspond to distinct types of energy, such as the distortional and dilatational types. Nevertheless, these findings are in accordance with remarks made by Rychlewski on purely theoretical grounds.

Moreover, applying the spectral decomposition principle on the compliance fourth-rank tensor $\mathbf{S}$, suitable for transversely isotropic plates, the stress $\boldsymbol{\sigma}$ second-rank tensor was analyzed in energy orthogonal states. Thus, the stress tensor $\boldsymbol{\sigma}$ on the principal stress plane (σ_1, σ_3) was specified altogether by two eigentensors $\overline{\boldsymbol{\sigma}_1}$ and $\overline{\boldsymbol{\sigma}_2}$, and these energy orthogonal stress states were proven to partition directly the elastic strain energy density in distinct constituents, $T_1(\boldsymbol{\sigma})$ and $T_2(\boldsymbol{\sigma})$. Moreover, it was shown that the $T_1(\boldsymbol{\sigma})$- and $T_2(\boldsymbol{\sigma})$-strain energies are associated with both shape distortions and alterations in volume of the medium, and depend on the value of the plane eigenangle ω_p, which, consequently, determines the type of strain energy stored. In the specialized case when the plane eigenangle ω_p equals either 45° or 135°, as in the case of isotropic media, the strain energy components become the distortional and dilatational types of energy. However, in the general case, the decomposition of the elastic potential, which is valid for the isotropic medium, is not valid for the transversely isotropic one.

On that account, the generalization of the decomposition of the total elastic strain energy density of isotropic media and cubic crystals into dilatational and distortional components seems unrealizable for the class of transversely isotropic media, because the spherical tensor $\mathbf{1}$ is not an eigentensor of the compliance tensor $\mathbf{S}$. Accordingly, the generalization of the Huber–von Mises–Hencky criterion in order

to hold for transversely isotropic plates and the introduction of the distortional energy as the critical failure quantity seems unfeasible.

Secondly, two loading paths were considered in loading the structure from the origin O to an arbitrary point F_n of the failure locus on the principal stress plane (σ_1, σ_3). However, it should be noted that the total energy expenditure is irrespective of the loading path, according to the principle of conservation of energy. The first loading path was a zigzag path (Fig. 6) along the directions parallel to the hydrostatic axis and its normal defined on the principal stress plane (σ_1, σ_3), passing through points O'' and F'', via the following routes:

$$OO'' \rightarrow O''F'' \rightarrow F''F_n. \tag{43}$$

Loading the plate from O to O'' along the first loading path, the energy expended is independent of the position of point F_n, being the same for all points of the EPFS, thus, reflecting the extent of anisotropy of the material. In addition, the OO'', $O''F''$, $F''F_n$ routes, involved in the first path, introduce two strain components, one in the normal, 'n', and one in the parallel 'p', direction. Therefore, the total elastic strain energy density $2\,T(\boldsymbol{\sigma}_{F_n})$ of the first path is equal to the sum of nine scalar products $\boldsymbol{\sigma}_i \cdot \boldsymbol{\epsilon}_i$, $i = \{\mathrm{p}, \mathrm{n}\}$, and may be decomposed into two orthogonal components, $T_{\mathrm{n}}(\boldsymbol{\sigma}_{F_n})$ and $T_{\mathrm{p}}(\boldsymbol{\sigma}_{F_n})$. The normal component, $T_{\mathrm{n}}(\boldsymbol{\sigma}_{F_n})$, refers to scalar products of stress and strain parallel to the hydrostatic axis, whereas the parallel component, $T_{\mathrm{p}}(\boldsymbol{\sigma}_{F_n})$, refers to scalar products normal to the hydrostatic axis, so that:

$$2T_{\mathrm{p}}(\boldsymbol{\sigma}_{F_n}) = \boldsymbol{\sigma}_{OO''} \cdot [(\boldsymbol{\epsilon}_{OO''})_{\mathrm{p}} + (\boldsymbol{\epsilon}_{O''F''})_{\mathrm{p}} + (\boldsymbol{\epsilon}_{F''F_n})_{\mathrm{p}}] + \boldsymbol{\sigma}_{F''F_n} \cdot [(\boldsymbol{\epsilon}_{OO''})_{\mathrm{p}} + (\boldsymbol{\epsilon}_{O''F''})_{\mathrm{p}} + (\boldsymbol{\epsilon}_{F''F_n})_{\mathrm{p}}], \tag{44a}$$

$$2T_{\mathrm{n}}(\boldsymbol{\sigma}_{F_n}) = \boldsymbol{\sigma}_{O''F''} \cdot [(\boldsymbol{\epsilon}_{\mathrm{OO}''})_{\mathrm{n}} + (\boldsymbol{\epsilon}_{O''F''})_{\mathrm{n}} + (\boldsymbol{\epsilon}_{F''F_n})_{\mathrm{n}}]. \tag{44b}$$

As a result, this splitting of the elastic strain energy density is a very favorable one, because the two strain energy components do not interfere. However, $T_{\mathrm{n}}(\boldsymbol{\sigma}_{F_n})$ and $T_{\mathrm{p}}(\boldsymbol{\sigma}_{F_n})$ are mixed types of energy, that is both dilatational and distortional, and do not correspond to distinct types of energy.

The second loading path (Fig. 7) was equivalent to the first one, crossing points O'' and F'', but along the directions of the $\overline{\boldsymbol{\sigma}_1}$- and $\overline{\boldsymbol{\sigma}_2}$-stress eigenstates. The latter were defined according to the spectral decomposition of the compliance $\mathbf{S}$ fourth-rank tensor for transversely isotropic plates. Thus, the second path comprised of the following routes:

$$OM'' \rightarrow M''O'' \rightarrow O''K'' \rightarrow K''F'' \rightarrow F''L'' \rightarrow L''F_n. \tag{45}$$

The total elastic strain energy density $2\,T(\boldsymbol{\sigma}_{F_n})$ of the second path is equal to the sum of the nineteen scalar products $\overline{\boldsymbol{\sigma}_i} \cdot \boldsymbol{\epsilon}_i$, $i = \{1, 2\}$, and may be split into two orthogonal components, $T_1(\boldsymbol{\sigma}_{F_n})$ and $T_2(\boldsymbol{\sigma}_{F_n})$. Component $T_1(\boldsymbol{\sigma}_{F_n})$ refers to scalar products of stress and strain in the direction of the $\overline{\boldsymbol{\sigma}_1}$-stress eigenstate, whereas component $T_2(\boldsymbol{\sigma}_{F_n})$ refers to scalar products in the direction of the $\overline{\boldsymbol{\sigma}_2}$-stress eigenstate, namely:

$$\begin{aligned} T_1(\boldsymbol{\sigma}_{F_n}) = {} & (\boldsymbol{\sigma}_{OM''})_1 \cdot [(\boldsymbol{\epsilon}_{OM''})_1 + (\boldsymbol{\epsilon}_{O''K''})_1 + (\boldsymbol{\epsilon}_{F''L''})_1] + (\boldsymbol{\sigma}_{O''K''})_1 \cdot [(\boldsymbol{\epsilon}_{OM''})_1 + (\boldsymbol{\epsilon}_{O''K''})_1 \\ & + (\boldsymbol{\epsilon}_{F''L''})_1] + (\boldsymbol{\sigma}_{F''L''})_1 \cdot [(\boldsymbol{\epsilon}_{OM''})_1 + (\boldsymbol{\epsilon}_{O''K''})_1 + (\boldsymbol{\epsilon}_{F''L''})_1], \end{aligned} \tag{46a}$$

$$T_2(\boldsymbol{\sigma}_{F_n}) = (\boldsymbol{\sigma}_{M''O''})_2 \cdot [(\boldsymbol{\epsilon}_{M''O''})_2 + (\boldsymbol{\epsilon}_{K''F''})_2 + (\boldsymbol{\epsilon}_{L''F_n})_2] + (\boldsymbol{\sigma}_{K''F''})_2 \cdot [(\boldsymbol{\epsilon}_{M''O''})_2 + (\boldsymbol{\epsilon}_{K''F''})_2 + (\epsilon_{L''F_n})_2] + (\boldsymbol{\sigma}_{L''F_n})_2 \cdot [(\boldsymbol{\epsilon}_{M''O''})_2 + (\boldsymbol{\epsilon}_{K''F''})_2 + (\boldsymbol{\epsilon}_{L''F_n})_2], \tag{46b}$$

in which the subscripts 1 and 2 represent the $\overline{\boldsymbol{\sigma}_1}$- and $\overline{\boldsymbol{\sigma}_2}$-eigenstates.

Finally, a third loading path may be considered (Fig. 7), which consists of two routes in the directions of the stress-eigenstates $\overline{\boldsymbol{\sigma}_1}$ and $\overline{\boldsymbol{\sigma}_2}$ of the transversely isotropic plate, namely:

$$OQ'' \rightarrow Q''F_n. \tag{47}$$

The elastic strain energy 2 $T(\boldsymbol{\sigma}_{F_n})$ of the third path is equal to the sum of two scalar products $\overline{\boldsymbol{\sigma}_i} \cdot \boldsymbol{\epsilon}_i$, $i = \{1, 2\}$. Thus, the strain energy in the principal stress plane (σ_1, σ_3) may be resolved in two components, $T_1(\boldsymbol{\sigma}_{F_n})$ and $T_2(\boldsymbol{\sigma}_{F_n})$, each one associated with one of the two stress eigenstates:

$$T_1(\boldsymbol{\sigma}_{F_n}) = (\boldsymbol{\sigma}_{OQ''})_1 \cdot (\boldsymbol{\epsilon}_{OQ''})_1, \tag{48a}$$

$$T_2(\boldsymbol{\sigma}_{F_n}) = (\boldsymbol{\sigma}_{Q''F_n})_2 \cdot (\boldsymbol{\epsilon}_{Q''F_n})_2, \tag{48b}$$

where the subscripts 1 and 2 denote the $\overline{\boldsymbol{\sigma}_1}$- and $\overline{\boldsymbol{\sigma}_2}$-states of stress.

Concluding, the last loading path is the most appropriate one in comparison to the other two, since the computation of the strain energy density of any point F_n on the failure locus involves less computations, that is only two scalar products compared to nine and eighteen scalar products involved in the first and second paths.

At last, it may be stated that for a thin plate of a transversely isotropic material, whose principal stress axes coincide with the principal material directions of the medium, it is always possible to decompose the total elastic strain energy density into two orthogonal components, in the sense of the scalar products of their associated stress states. Furthermore, the decomposition of the strain energy is advantageous, based on the fact that the two strain energy parts are non-interacting, such that one does not interfere with the other.

References

Coulomb, C.A., 1773. Essai sur l'application des regles des maximis et minimis a quelques problemes de statique relatifs a l'architecture. Memoires de Mathematiques et de Physique, Acad. Roy. Des Sciences par divers savants 7, 343–382.

Hill, R., 1948. A theory of yielding and plastic flow of anisotropic metals. Proc. Roy. Soc. Lond. A193, 281–297.

Hoffman, O., 1967. The brittle strength of orthotropic materials. J. Comp. Mat. 1, 200–206.

Lekhnitskii, S., 1963. Theory of Elasticity of an Anisotropic Elastic Body. Holden-Day, San Francisco Translated by P. Fern.

Olszak, W., Urbanowski, W., 1956. The plastic potential and the generalized distortion energy in the theory of nonhomogeneous anisotropic elastic–plastic bodies. Arch. Mekh. Stos. 8, 671–694.

Olszak, W., Ostrowska-Maciejewska, J., 1985. The plastic potential in the theory of anisotropic elastic–plastic solids. Engng Fract. Mech. 21 (4), 625–632.

Rychlewski, J., 1984a. Elastic energy decompositions and limit criteria. Advances in Mech. 7 (3), 51–80.

Rychlewski, J., 1984b. On Hooke's law. PMM 48 (3), 303–314.

Srinivasan, T.P., Nigam, S.D., 1969. Invariant elastic constants for crystals. J. Math. Mech. 19 (5), 411–420.

Theocaris, P.S., 1986. Failure criteria for engineering materials based on anisotropic hardening. Proc. Nat. Acad. Athens 61 (1), 84–114.

Theocaris, P.S., 1987a. Failure characterization of anisotropic materials by means of the elliptic paraboloid failure surface. Uspechi Mekhanikii (Advances in Mechanics) 10, 83–102.

Theocaris, P.S., 1987b. Failure criteria in fiber composites. Proc. Nat. Acad. Athens 62 (1), 129–142.

Theocaris, P.S., 1987c. Generalized failure criteria in the principle stress space. Proc. Bulg. Acad. Sci. (special issue). Theoretichna I Prilojnia Mekhanika (Theor. and Appl. Mech.) 19 (2), 74–104.

Theocaris, P.S., 1988a. Failure criteria for transtropic pressure dependent materials: the fiber composites. Rheol. Acta 27 (5), 451–465.

Theocaris, P.S., 1988b. The elliptic paraboloid failure surface for 2D-transtropic plates (fiber laminates). *Engng. Fract. Mech.* 33, 185–203.

Theocaris, P.S., 1989. The paraboloid failure surface for the general orthotropic material. Acta Mechanica 79 (1), 53–79.

Theocaris, P.S., 1994. Failure criteria for anisotropic bodies. In: Carpinteri, A. (Ed.), Handbook of Fatigue Crack Propagation in Metallic Structures, vol. 1. Elsevier, Amsterdam, pp. 3–45.

Theocaris, P.S., Philippidis, T.P., 1987. The paraboloidal failure surface of initially anisotropic elastic solids. J. Reinf. Plastics and Compos. 6, 378–395.

Theocaris, P.S., Philippidis, T.P., 1990. Variational bounds on the eigenvalue ω of transversely isotropic materials. Acta Mechanica 85 (1), 13–26.

Theocaris, P.S., Philippidis, T.P., 1991. Spectral decomposition of compliance and stiffness fourth-rank tensors suitable for orthotropic materials. Zeitsch. Angew. Math. and Mech. 71 (3), 161–171.

Theocaris, P.S., Sokolis, D.P., 1998. Spectral decomposition of the compliance tensor for anisotropic plates. J. Elasticity 51 (1), 89–103.

Tsai, S.W., Wu, E.M., 1971. A general theory of strength for anisotropic materials. J. Comp. Mat. 5, 58–80.

von Mises, R., 1928. Mechanik der plastischen Formanderung von Kristallen. Zeit. Ang. Math. und Mech. 8, 161–185.

Walpole, L.J., 1981. Elastic behaviour of composite materials: theoretical foundations. Adv. Appl. Mech. 21, 169–187.

Walpole, L.J., 1984. Fourth-rank tensors of the thirty-two crystal classes: multiplication tables. Proc. Roy. Soc. Lond. A391, 149–179.